Hindawi
Wireless Communications and Mobile Computing
Volume 2022, Article ID 2234458, 7 pages
https://doi.org/10.1155/2022/2234458

Research Article

Nonhomogeneous Data-Based Direct Position Determination: The RD-DPD-Capon Algorithm

Shengmei Luo,[1] Chao Wang,[1] Baobao Li,[2] and Gaofeng Zhao[2]

[1]*Nanjing Zhongfu Information Technology Co., Ltd, Nanjing 211800, China*
[2]*College of Electronic Information Engineering, Nanjing University of Aeronautics and Astronautics, Nanjing 211106, China*

Correspondence should be addressed to Gaofeng Zhao; zhaogaofeng@nuaa.edu.cn

Received 7 May 2022; Revised 27 June 2022; Accepted 4 July 2022; Published 27 July 2022

Academic Editor: Guimei Zheng

The accuracy of conventional two-step location methods is insufficient since the information loss problem in the parameter matching procedure. In this paper, we propose a Reduced Dimension Direct Position Determination with Capon (RD-DPD-Capon) algorithm. By introducing the idea of dimension reduction, the proposed algorithm avoids grid search along with the attenuation coefficient domain. Therefore, the RD-DPD-Capon algorithm has relatively low computational complexity. Meanwhile, the proposed algorithm inherits the high resolution and localization accuracy of the DPD-Capon algorithm. Numerical simulation verifies that the RD-DPD-Capon algorithm outperforms other conventional algorithms.

1. Introduction

With the rapid development of wireless communication and Internet of Things (IoT) techniques, the localization techniques of multisources based on antenna arrays has attracted a lot of attention [1, 2]. In many fields, such as radar, sonar, medicine, and vehicular technology, localization techniques are playing important roles [3].

At present, most traditional localization techniques for multiple sources consist of two independent processing steps [4]. The first step extracts intermediate parameters, such as time difference of arrival (TDOA), angle of arrival (AOA), and time of arrival (TOA), from the received signals [5–7]. Then, the second step establishes and solves a position equation according to the observation station position and measured intermediate parameters [8]. In addition, an additional source-parameter matching process is required between the two steps of the two-step algorithms [9]. However, the parameter matching process will fail if the source is too far from stations, and the clustering algorithm [10] must be used to eliminate false location points in the multisource location scenario. Due to the two steps being independent in each observation station, the constraint between intermediate parameters and sources is neglect, which leads the low accuracy and poor robustness [11].

As the electromagnetic environment becomes more and more complex, however, the demand for positioning accuracy in industrial applications is also increasing [12]. Traditional two-step methods can hardly be adapted to the environment due to the low accuracy and poor robustness, and it is urgent to develop the high accuracy localization technology to support the advance of industrial applications [13]. Aiming at the disadvantages of two-step methods, the Direct Positioning Determination (DPD) technology was proposed [14]. The DPD approaches have one-step localization from the received data and resultantly have improved accuracy. Although DPD algorithms also have the disadvantage of high requirements on hardware devices, with the rapid development of computing technology, this problem can be effectively overcome [15].

The deco-DPD algorithm generalized the DPD approaches into multiple source scene by performing the decoherent subspace decomposition in the cost function construction [16]. By measuring the time difference of arrival and their variances, the TA-DPD algorithm minimized the searching area and further solved the problem of

ship location based on the satellite platform [17]. Moreover, the Subspace Data Fusion (SDF) approach used a movable array to solve the problem of communication bandwidth [18]. The authors in [17] deduced the Optimal Weight Subspace Data Fusion (OWSDF) in the Gaussian noise environment [19]. For the sake of increasing sources that can be located, Ref [20] proposed a new DPD algorithm using the cross-correlation matrix (CCM). Similarly, Oispuu and Nickel [21] presented a Capon-based DPD method, which can locate more sources than the number of elements in a single array. In order to improve the resolution for wake sources, DPD-MVDR combined the idea of the Minimum Variance Distortionless Response (MVDR) estimator and DPD. However, the DPD-MVDR approach has very high computational complexity and faces significant performance degradation at the low signal-to-noise ratio (SNR) [22].

In this paper, we focus on the directly localizing of multiple sources and propose a Reduced Dimension Direct Position Determination with Capon (RD-DPD-Capon) algorithm. Firstly, we build the received signal model, which takes into account the actual path fading and antenna gain, aiming at multiple source localization scene. Then, we construct the covariance matrix of the received signals from multiple distributed arrays to integrally localize sources. Finally, we construct the cost function, which avoids grid search along with the attenuation coefficient domain, to reduce computational complexity. In summary, the main contributions of this paper are as follows:

(1) We proposed a reduced dimension Capon-based DPD algorithm, which avoids the grid research along with attenuation coefficient and remarkably reduces computational complexity

(2) We compare the proposed algorithm with the traditional AOA two-step location method and the DPD-Capon algorithm via numerical simulations. Simulation results verify that the RD-DPD-Capon algorithm outperforms other conventional algorithms

Notations: $(\cdot)^{-1}$, $(\cdot)^T$, and $(\cdot)^H$ denote inversion, transposition, and conjugate transposition of matrix, respectively. $\|\cdot\|_2$ means the 2-norm of a vector, and ∂ is partial derivation. $\mathscr{E}\{\cdot\}$ represents the mathematical expectation, and $\hat{\mathbf{R}}$ denotes the estimation of $\mathbf{R}$. diag $\{\mathbf{a}\}$ denotes the diagonal matrix consisted of all elements of vector $\mathbf{a}$.

2. Problem Formulation

Considering the localization geometry illustrated in Figure 1, Q far-field sources locate at $\mathbf{v}_1, \mathbf{v}_2, \cdots, \mathbf{v}_Q$, where $\mathbf{v}_q = [v_{x,q}, v_{y,q}]^T$. L observation stations with precisely known locations, $\mathbf{u}_1, \mathbf{u}_2, \cdots, \mathbf{u}_L$, are separately distributed in the space, where $\mathbf{u}_q = [u_{x,q}, u_{y,q}]^T$. Assume each station is equipped with a uniform line array of M elements, and denote the position coordinate of the m-th sensor of the

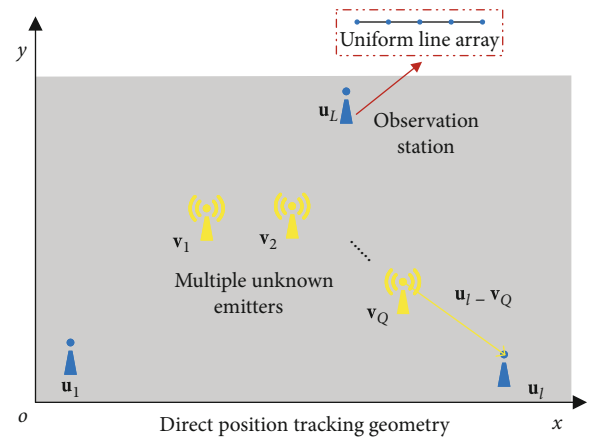

Figure 1: Localization geometry.

l-th station as $\mathbf{d}_{m,l} = [d_{x,m,l}, d_{y,m,l}, d_{z,m,l}]^T$. The received signal of the l-th observation station is [19]

$$\mathbf{x}_l(t) = \mathbf{A}_l \mathbf{s}_l(t) + \mathbf{n}_l(t), \tag{1}$$

where $\mathbf{s}_l(t) = [s_{1,l}(t), \cdots, s_{Q,l}(t)]^T$ contains the received envelope of Q signals. $\mathbf{n}_l(t)$ represents independent additive Gaussian white noise, where the mean is zero and the variance is σ_n^2. $\mathbf{A}_l = [\alpha_{1,l}\mathbf{a}_{1,l}, , \cdots, \alpha_{Q,l}\mathbf{a}_{Q,l}]$ denotes the manifold matrix, where $\boldsymbol{\alpha}_{q,l}$ means the influence of path fading and receive gain and $\mathbf{a}_{1,l}(t)$ is given by [19]

$$\mathbf{a}_{ql}(t) = \left[1, e^{j\mathbf{k}_{ql}^T(\mathbf{d}_{1,l} - \mathbf{d}_{0,l})}, \cdots, e^{j\mathbf{k}_{ql}^T(\mathbf{d}_{M-1,l} - \mathbf{d}_{0,l})}\right]^T, \tag{2}$$

where $\mathbf{d}_{m,l} = [d_{m,x,l}, d_{m,y,l}, d_{m,z,l}]^T$ is the position vector of the m-th element and $\mathbf{k}_{q,l}$ is the wavenumber

$$\mathbf{k}_{q,l} = \frac{2\pi}{\lambda} \frac{\mathbf{v}_q - \mathbf{u}_l}{\|\mathbf{v}_q - \mathbf{u}_l\|_2}. \tag{3}$$

The combination of the received signal of L stations is given by

$$\mathbf{x}(t) = \mathbf{A}\mathbf{s}(t) + \mathbf{n}(t), \tag{4}$$

where $\mathbf{s}(t) = [\mathbf{s}_1^T(t), \cdots, \mathbf{s}_L^T(t)]^T$ and $\mathbf{n}(t) = [\mathbf{n}_1^T(t), \cdots, \mathbf{n}_L^T(t)]^T$. The fused array manifold matrix $\mathbf{A}$ is given by

$$\mathbf{A} = \begin{bmatrix} \mathbf{A}_1 & & & \\ & \mathbf{A}_2 & & \\ & & \ddots & \\ & & & \mathbf{A}_L \end{bmatrix}. \tag{5}$$

The autocorrelation of $\mathbf{x}(t)$ can be expressed by [6]

$$\begin{aligned}\mathbf{R} &= \mathscr{E}\{\mathbf{x}(t)\mathbf{x}^H(t)\} = \mathbf{A}\mathscr{E}\{\mathbf{s}(t)\mathbf{s}^H(t)\}\mathbf{A}^H + \sigma_n^2\mathbf{I}_{ML} \\ &= \mathbf{A}\mathbf{R}_{ss}\mathbf{A}^H + \sigma_n^2\mathbf{I}_{ML},\end{aligned} \tag{6}$$

where $\mathbf{R}_{ss} = \mathscr{E}\{\mathbf{s}(t)\mathbf{s}^H(t)\}$. In practice, $\mathbf{R}$ is usually measured from limited J snapshots

$$\hat{\mathbf{R}} = \sum_{n=1}^{J} \mathbf{x}(nT)\mathbf{x}^H(nT), \tag{7}$$

where T is the sampling period.

3. The RD-DPD-Capon Algorithm

Based on matrix eigenvalue decomposition theory [18], $\mathbf{R}$ can be rewritten as

$$\begin{aligned}&\mathbf{R} = \mathbf{E}\boldsymbol{\Sigma}\mathbf{E}^H = \sum_{i=1}^{ML} \lambda_i e_i e_i^H, \\ &\mathbf{E} = \left[e_1, \cdots, e_Q\right], \\ &\boldsymbol{\Sigma} = \text{diag}\left\{\lambda_1, \lambda_2, \cdots, \lambda_{ML}\right\},\end{aligned} \tag{8}$$

where unitary matrix $\mathbf{E}$ comprises ML eigenvectors of $\mathbf{R}$ and $\boldsymbol{\Sigma}$ contains ML eigenvalues. Eigenvector e_i and eigenvalue λ_i come in pairs. In addition, we assume the eigenvalues in the order of $\lambda_1 \geq \lambda_2 \geq \cdots \geq \lambda_Q \geq \lambda_{Q+1} = \cdots = \lambda_{ML} = \sigma_n^2$, where the eigenvectors corresponding to Q larger eigenvalues span the same linear space as the array manifold.

$$\mathbf{E}_s = \left[e_1, \cdots, e_Q\right] = \mathbf{A}\mathbf{T}, \tag{9}$$

where $\mathbf{T}$ is an invertible basis change matrix. It is straightforwardly to deduce that

$$\mathbf{R}^{-1} = \mathbf{E}\boldsymbol{\Sigma}^{-1}\mathbf{E}^H = \sum_{i=1}^{ML} \lambda_i^{-1} e_i e_i^H. \tag{10}$$

Obviously, $1/\lambda_1 \leq 1/\lambda_2 \leq \cdots \leq 1/\lambda_Q \leq 1/\lambda_{Q+1} = \cdots = 1/\lambda_{ML} = 1/\sigma_n^2$. We can localize sources by finding the Q minimums of the DPD-Capon cost function [21].

$$f_{\text{Capon}} = \mathbf{b}_s^{\text{H}}\mathbf{R}^{-1}\mathbf{b}_s, \tag{11}$$

where $\mathbf{b}_s = \left[\mathbf{a}_1^T(\mathbf{v}_s)\alpha_1, \cdots, \mathbf{a}_L^T(\mathbf{v}_s)\alpha_L\right]^T$ and $\mathbf{v}_s = [v_x, v_y]^T$ denotes the potential positions of sources. However, $\mathbf{b}_s$ contains extra unknown attenuation coefficient $\alpha_1, \alpha_2, \cdots, \alpha_L$, which will lead complex $L+2$ dimension search. Due to the fact that most practical applications are not interested in path fading, we propose a cost function that excludes dimension search for fading coefficients. Expand $\mathbf{b}_s$ as

$$\begin{aligned}\mathbf{b}_s &= \left[\mathbf{a}_1^T(\mathbf{v}_s)\alpha_1, \cdots, \mathbf{a}_L^T(\mathbf{v}_s)\alpha_L\right]^T \\ &= \begin{bmatrix} \mathbf{a}_1(\mathbf{v}_s) & & & \\ & \mathbf{a}_2(\mathbf{v}_s) & & \\ & & \ddots & \\ & & & \mathbf{a}_L(\mathbf{v}_s) \end{bmatrix} \begin{bmatrix} \alpha_1 \\ \alpha_2 \\ \vdots \\ \alpha_L \end{bmatrix} = \mathbf{A}_s\boldsymbol{\alpha}.\end{aligned} \tag{12}$$

Furthermore, we add a constraint of $\mathbf{e}^H\boldsymbol{\alpha} = 1$ to eliminate the trivial solution of all zeros $\boldsymbol{\alpha}$, where $\mathbf{e} = [1, 0, \cdots, 0]^T$. Then, the cost function is rewritten as [23]

$$\arg\min_{\mathbf{v}_s} \boldsymbol{\alpha}^H\mathbf{A}_s^H(\mathbf{v}_s)\mathbf{R}^{-1}\mathbf{A}_s(\mathbf{v}_s)\boldsymbol{\alpha}, \quad \text{s.t.}\mathbf{e}^H\boldsymbol{\alpha} = 1. \tag{13}$$

Define $\mathbf{Q}(\mathbf{v}_s) = \mathbf{A}_s^H(\mathbf{v}_s)\mathbf{R}^{-1}\mathbf{A}_s(\mathbf{v}_s)$ and substitute it into (12), and we find

$$\arg\min_{\mathbf{v}_s} \boldsymbol{\alpha}^H\mathbf{Q}(\mathbf{v}_s)\boldsymbol{\alpha}, \quad \text{s.t.}\mathbf{e}^H\boldsymbol{\alpha} = 1. \tag{14}$$

Subsequently, we construct new cost function Lagrange multiplier method

$$L(\mathbf{v}_s, \boldsymbol{\alpha}) = \boldsymbol{\alpha}^H\mathbf{Q}(\mathbf{v}_s)\boldsymbol{\alpha} - \lambda\left(\mathbf{e}^H\boldsymbol{\alpha} - 1\right), \tag{15}$$

where λ is a deterministic constant. Seek partial derivative

$$\frac{\partial}{\partial(\boldsymbol{\alpha})} L(\mathbf{v}_s, \boldsymbol{\alpha}) = 2\mathbf{Q}(\mathbf{v}_s)\boldsymbol{\alpha} + \lambda\mathbf{e} = 0. \tag{16}$$

Clearly, we have $\boldsymbol{\alpha} = -\lambda\mathbf{Q}^{-1}(\mathbf{v}_s)\mathbf{e}/2$. Consider $\mathbf{e}^H\boldsymbol{\alpha} = 1$,

$$\boldsymbol{\alpha} = \frac{(\mathbf{Q}(\mathbf{v}_s))^{-1}\mathbf{e}}{\mathbf{e}^H(\mathbf{Q}(\mathbf{v}_s))^{-1}\mathbf{e}}. \tag{17}$$

Substitute (16) back into (12), we can finally give the cost function without $\boldsymbol{\alpha}$.

$$\arg\min_{\mathbf{v}_s} \frac{1}{\mathbf{e}^H(\mathbf{Q}(\mathbf{v}_s))^{-1}\mathbf{e}} = \arg\max_{\mathbf{v}_s} \mathbf{e}^H(\mathbf{Q}(\mathbf{v}_s))^{-1}\mathbf{e}. \tag{18}$$

Table 1: Complexity comparison of DPD-Capon algorithm and RD-DPD-Capon algorithm.

Algorithms	Computational complexity
DPD-Capon	$O\left(M^3L^3 + JM^2L^2 + F_xF_yF_\alpha^L ML^3(M+1)\right)$
RD- DPD-Capon	$O\left(M^3L^3 + JM^2L^2 + F_xF_yML^3(M+1)\right)$

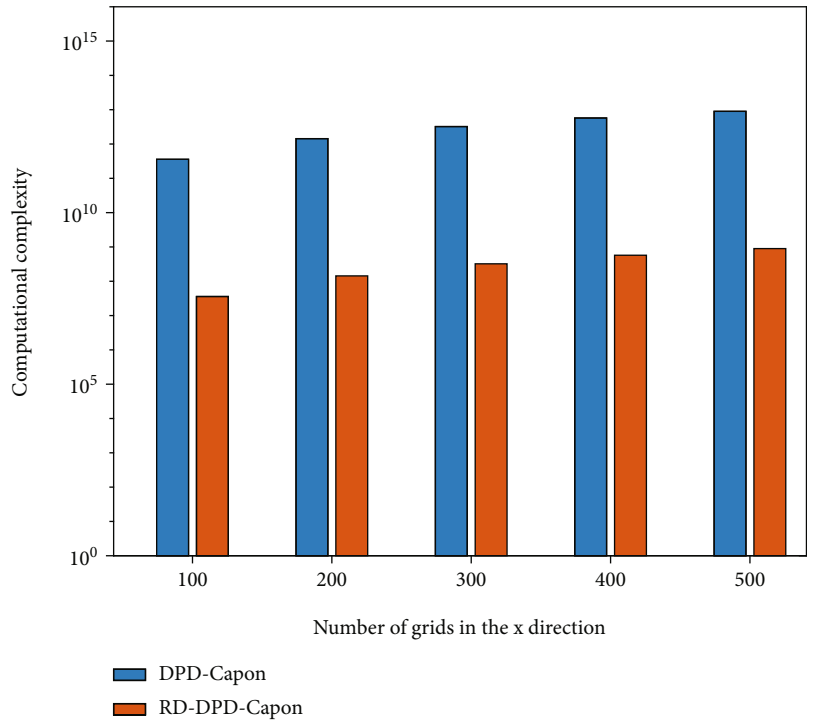

Figure 2: Complexity comparison of algorithms DPD-Capon and RD-DPD-Capon.

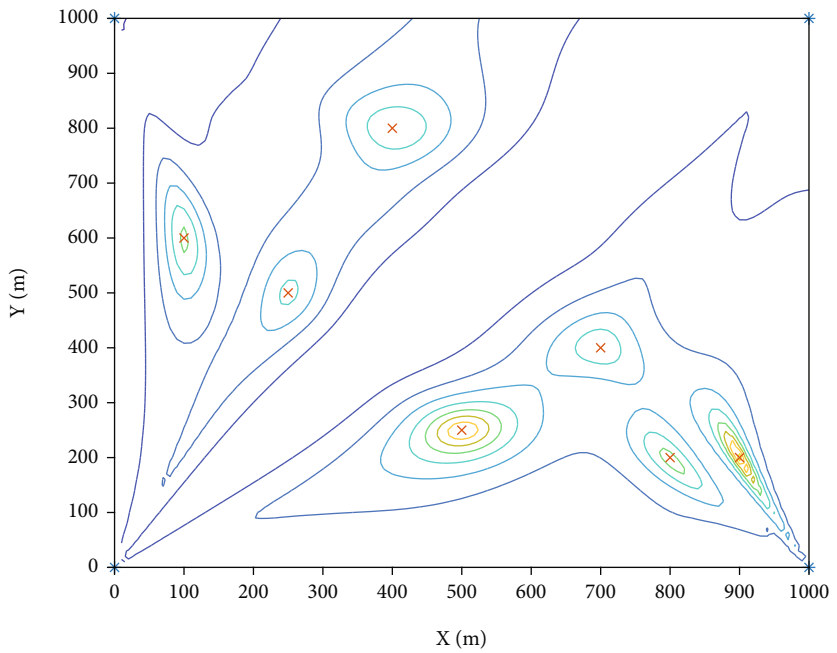

Figure 3: Contour map of RD-DPD-Capon algorithm localization results.

Finally, we can determinate all Q sources by searching the Q maximums of the $(1, 1)$-th element of $\mathbf{Q}^{-1}(\mathbf{p})$ [23].

The organized steps of the RD-DPD-Capon algorithm are displayed as follows:

(1) For each station, observe signals and sample J snapshots, and get $\mathbf{x}_l(t), t = 1, \cdots, J$

(2) Fuse the received data of L stations to construct $\mathbf{x}(t)$, $t = 1, \cdots, J$

(3) Calculate the covariance matrix of fused data via (7)

(4) Compute the inverse of the covariance matrix

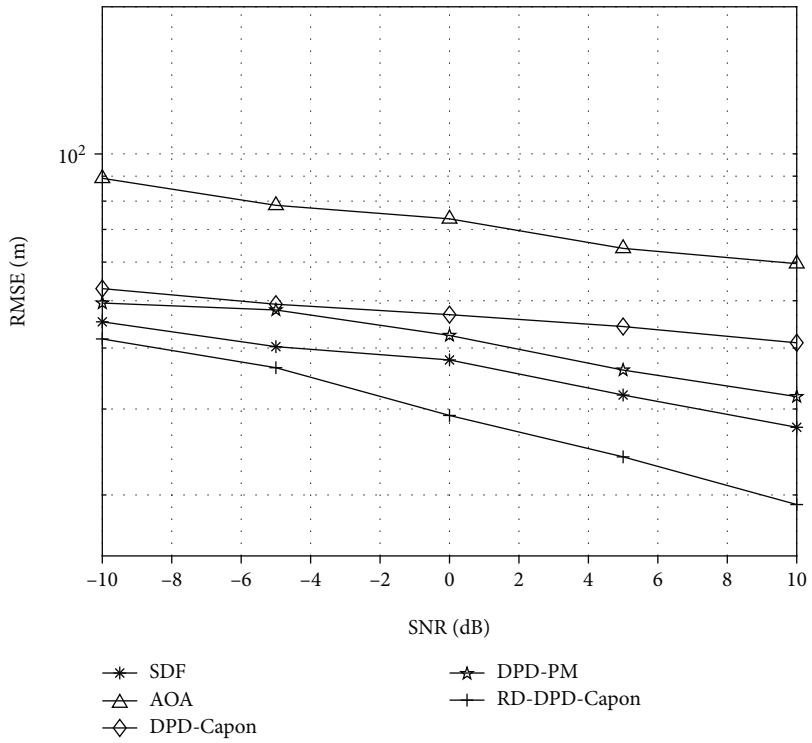

Figure 4: Performance comparison versus SNR (different algorithms).

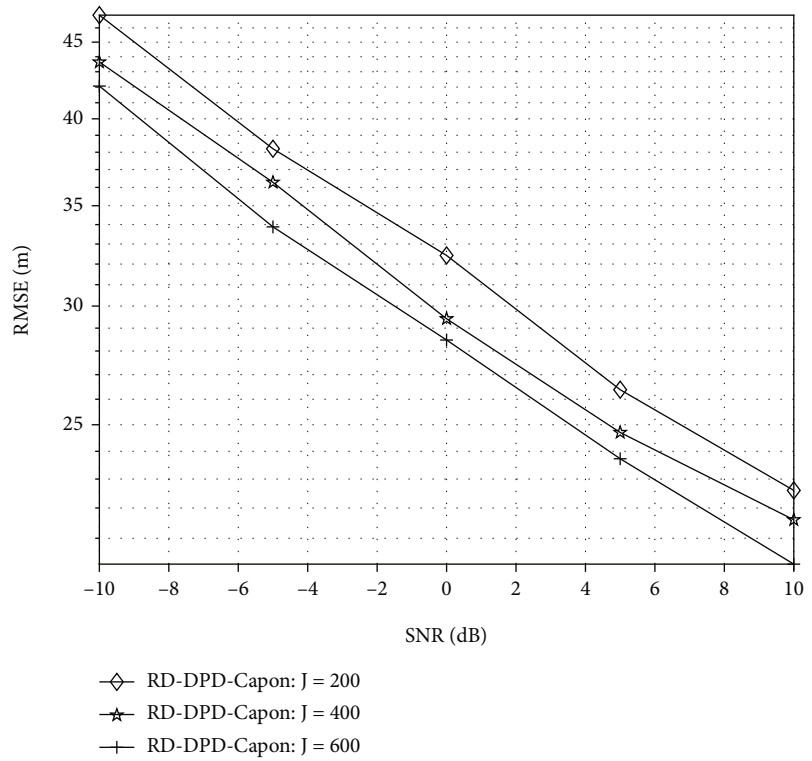

Figure 5: Performance comparison versus SNR (different snapshots).

(5) Calculate the value of the cost function at each 2D grid according to (18)

(6) Determine the position of Q sources by finding the position corresponding to the largest Q peaks of the cost function

(7) Substitute the estimated position of sources into (17) to determine the attenuation coefficients $\widehat{\alpha}_1$, $\widehat{\alpha}_2, \cdots, \widehat{\alpha}_L$

4. Complexity Analysis

This section analyses and compares the complexity of algorithms DPD-Capon [21] and RD-DPD-Capon, where the number of multiple times is considered. The complexities are related to the number of signals Q, the number of stations L, array elements M, and the number of search grids along the x and y directions, which are denoted as F_x and F_y. Table 1 summarizes the closed-form expression of the computational complexities of algorithms DPD-Capon and RD-DPD-Capon. Figure 2 compares the complexities of two algorithms under logarithmic axis. The grid number is along the x direction and y direction, from 100 to 500, and other parameters are set as follows: the number of snapshots $J = 100$, the number of array elements $M = 7$, the number of arrays $L = 4$, and the number of signals $Q = 3$. As are shown in table and figure, the RD-DPD-Capon algorithm has remarkably lower complexity than DPD-Capon algorithm. The reason is that the RD-DPD-Capon algorithm avoids the grid search along attenuation coefficient direction.

5. Simulation Results

This section uses Monte Carlo experiments to analyse the localization performance of the proposed algorithm, where Root Mean Square Error (RMSE) is the measurement standard, which is defined as follows:

$$\mathrm{RMSE} = \frac{1}{Q}\sqrt{\frac{1}{\mathrm{MC}}\sum_{\mathrm{mc}=1}^{\mathrm{MC}}\sum_{q=1}^{Q}\left\|\mathbf{v}_q - \widehat{\mathbf{v}}_{q,\mathrm{mc}}\right\|_2^2}, \tag{19}$$

where MC denotes the total number of Monte Carlo simulations and $\widehat{\mathbf{v}}_{q,\mathrm{mc}}$ means the estimates of $\mathbf{v}_q$ in the mc-th trial. In following simulations, MC = 1000.

Figure 3 is the contour map of RD-DPD-Capon algorithm localization results, where the signal-to-noise ratio (SNR) is 10 dB, the number of sources $Q = 2$, and the positions of stations are (0, 0), (0, 1000 m), (1000 m, 0), and (1000 m, 1000 m). In addition, the positions of sources are given by (100 m, 600 m), (250 m, 500 m), (400 m, 800 m), (700 m, 400 m), (500 m, 250 m), (800 m, 200 m), and (900 m, 200 m), respectively. Each station contains a 7-element uniform linear array and sample 500 snapshots per observation. From the contour map, it can be observed that all sources are correctly localized, which verifies that the proposed algorithm can localize multiple sources with well performance.

Figure 4 compares the localization performance of the proposed algorithm with that of other algorithms, where SNR varies from -10 dB to 10 dB. The algorithms SDF [18], AOA-based two-step method [7, 10], DPD-Capon [21], and DPD-PM are taken into account. Besides, the sources and AOA parameters are assumed ideally matched in this section. Consider 3 sources locate at (400 m, 200 m), (200 m, 700 m), and (600 m, 400 m), respectively. Different from Figure 4, Figure 5 considers 4 sources, which locate at (400 m, 200 m), (200 m, 700 m), (600 m, 400 m), and (300 m, 400 m). As are shown in figures, the localization performance of all these algorithms improves as SNR increases. It is obvious that the proposed RD-DPD-Capon algorithm outperforms other algorithms.

6. Conclusion

In this paper, we discuss the simultaneous localization of multiple unknown sources and proposed the RD-DPD-Capon algorithm. The proposed algorithm has lower complexity since it avoids grid search along with the attenuation coefficient domain. Meanwhile, the localization accuracy is guaranteed by fusing and integrally processing the observed data of all distributed stations. Compared with the other conventional DPD methods, our RD-DPD-Capon algorithm has higher localization accuracy for multisource locations.

Data Availability

The research in this paper is based on theoretical derivation and numerical simulation, and there is no experimental data to share.

Conflicts of Interest

The authors declare that there is no conflict of interest.

Acknowledgments

This study was funded by the State Key Laboratory of Marine Resource Utilization in South China Sea (Hainan University) (MRUKF2021033), the Sonar Technology Key Laboratory (Range estimation and location technology of passive target via multiple array combination), the Jiangsu Planned Projects for Postdoctoral Research Funds (2020Z013), and the China Postdoctoral Science Foundation (2020M681585).

References

[1] P. N. Beuchat, H. Hesse, A. Domahidi, and J. Lygeros, "Enabling optimization-based localization for IoT devices," *IEEE Internet of Things Journal*, vol. 6, no. 3, pp. 5639–5650, 2019.

[2] N. Bni Lam, D. Joosens, M. Aernouts, J. Steckel, and M. Weyn, "LoRay: AoA estimation system for long range communication networks," *IEEE Transactions on Wireless Communications*, vol. 20, no. 3, pp. 2005–2018, 2021.

[3] A. B. C. da Silva, S. K. Joshi, S. V. Baumgartner, F. Q. de Almeida, and G. Krieger, "Phase correction for accurate

DOA angle and position estimation of ground-moving targets using multi-channel airborne radar," *IEEE Geoscience and Remote Sensing Letters*, vol. 19, article 4021605, pp. 1–5, 2022.

[4] Q. Zhu, H. Li, Y. Fu et al., "A novel 3D non-stationary wireless MIMO channel simulator and hardware emulator," *IEEE Transactions on Communications*, vol. 66, no. 9, pp. 3865–3878, 2018.

[5] X. Wu, W. Zhu, J. Yan, and Z. Zhang, "A spatial filtering based gridless DOA estimation method for coherent sources," *IEEE Access*, vol. 6, pp. 56402–56410, 2018.

[6] Z. Zheng, Y. Huang, W. Wang, and H. C. So, "Spatial smoothing PAST algorithm for DOA tracking using difference oarray," *IEEE Signal Processing Letters*, vol. 26, no. 11, pp. 1623–1627, 2019.

[7] S. Kim, D. Oh, and J. Lee, "Joint DFT-ESPRIT estimation for TOA and DOA in vehicle FMCW radars," *IEEE Antennas and Wireless Propagation Letters*, vol. 14, pp. 1710–1713, 2015.

[8] D. Liu, K. Liu, Y. Ma, and J. Yu, "Joint TOA and DOA localization in indoor environment using virtual stations," *IEEE Communications Letters*, vol. 18, no. 8, pp. 1423–1426, 2014.

[9] Y. Li, S. Li, Q. Song, H. Liu, and M. Q. H. Meng, "Fast and robust data association using posterior based approximate joint compatibility test," *IEEE Transactions on Industrial Informatics*, vol. 10, no. 1, pp. 331–339, 2014.

[10] Z. Yang, C. Liu, and L. Jin, "A clustering-based algorithm for device-free localization in IoT," in *2018 IEEE 4th International Conference on Computer and Communications (ICCC)*, pp. 769–773, Chengdu, China, 2018.

[11] A. Amar and A. J. Weiss, ""Analysis of direct position determination approach in the presence of model errors," IEEE/SP 13th Workshop on Statistical," *Signal Processing*, vol. 2005, pp. 521–524, 2005.

[12] T. Van Haute, B. Verbeke, E. De Poorter, and I. Moerman, "Optimizing time-of-arrival localization solutions for challenging industrial environments," *IEEE Transactions on Industrial Informatics*, vol. 13, no. 3, pp. 1430–1439, 2017.

[13] L. Sun, L. Wan, and X. Wang, "Learning-based resource allocation strategy for industrial IoT in UAV-enabled MEC systems," *IEEE Transactions on Industrial Informatics*, vol. 17, no. 7, pp. 5031–5040, 2021.

[14] A. J. Weiss, "Direct geolocation of wideband emitters based on delay and Doppler," *IEEE Transactions on Signal Processing*, vol. 59, no. 6, pp. 2513–2521, 2011.

[15] A. Londhe, V. Bhalerao, S. Ghodey, S. Kate, N. Dandekar, and S. Bhange, "Data division and replication approach for improving security and availability of cloud storage," *Fourth International Conference on Computing Communication Control and Automation (ICCUBEA)*, vol. 2018, pp. 1–4, 2018.

[16] A. Amar and A. J. Weiss, "Direct position determination (DPD) of multiple known and unknown radio-frequency signals," in *2004 12th European Signal Processing Conference*, pp. 1115–1118, Vienna, Austria, 2004.

[17] S. Li, Q. Zhang, B. Deng, B. Wu, and Y. Gao, "A fast and accurate LEO satellite-based direct position determination assisted by TDOA measurements," *China Communications*, vol. 19, no. 1, pp. 92–103, 2022.

[18] B. Demissie, M. Oispuu, and E. Ruthotto, "Localization of multiple sources with a moving array using subspace data fusion," in *2008 11th International Conference on Information Fusion*, pp. 1–7, Cologne, Germany, 2008.

[19] J. Li, Y. He, X. Zhang, and Q. Wu, "Simultaneous localization of multiple unknown emitters based on UAV monitoring big data," *IEEE Transactions on Industrial Informatics*, vol. 17, no. 9, pp. 6303–6313, 2021.

[20] G. Wang, C. Gao, S. G. Razul, and C. M. S. See, "A new direct position determination algorithm using multiple arrays," in *2018 IEEE 23rd International Conference on Digital Signal Processing (DSP)*, pp. 1–5, Shanghai, China, 2018.

[21] M. Oispuu and U. Nickel, "Direct detection and position determination of multiple sources with intermittent emission," *Signal Processing*, vol. 90, no. 12, pp. 3056–3064, 2010.

[22] T. Tirer and A. J. Weiss, "High resolution direct position determination of radio frequency sources," *IEEE Signal Processing Letters*, vol. 23, no. 2, pp. 192–196, 2016.

[23] X. Zhang, L. Xu, L. Xu, and D. Xu, "Direction of departure (DOD) and direction of arrival (DOA) estimation in MIMO radar with reduced-dimension MUSIC," *IEEE Communications Letters*, vol. 14, no. 12, pp. 1161–1163, 2010.